Mathematics Today Vol.34(A) (April 2018 – Special Issue) 100-114
ISSN 0976-3228, e-ISSN 2455-9601

Radiative Effect on Parabolic Motion of Casson Fluid Flow Past Over Vertical Plate Embedded in a Porous Medium

Mr. Rahul P. Mehta[1], Dr. Hari R. Kataria[2]

[1]Applied Science & Humanities Department,
Sardar Vallabhbhai Patel Institute of Technology, Vasad, India
[1]rahul1078@gmail.com
Corresponding author[1] (+91-9898066500)

[2]Department of Mathematics, Faculty of Science,
The M. S. University of Baroda, Vadodara, India
[2]hrkrmaths@yahoo.com

Abstract

This article studies radiative and parabolic motion effects on unsteady MHD flow of Casson fluid past a vertical plate with ramped wall temperature. The fluid is electrically conducting and passing through a porous medium. This phenomenon is modeled in the form of partial differential equations with initial and boundary conditions. Some suitable non-dimensional variables are introduced. The corresponding dimensionless equations with conditions are solved using the Laplace transform technique. Analytical expressions for velocity, temperature and concentration profiles are obtained. The features of the velocity, temperature and concentration are analyzed by plotting graphs and the physical aspects are studied for different parameters like the magnetic field parameter, radiation parameter, chemical reaction parameter, thermal Grashof number and time.

Keywords: MHD; Casson fluid; Parabolic Motion
AMS Subject Classification: 76W05, 76S05

Nomenclature:

B_0 Uniform magnetic field	R Thermal Radiation
C' Species concentration	θ Dimensionless fluid temperature
D_M Mass diffusion coefficient	u Dimensionless fluid velocity in x direction
D_T Thermal diffusion coefficient	C Dimensionless species concentration
Gm Mass Grashof number	C_p Specific heat at constant pressure
k Permeability parameter	g Acceleration due to gravity
k_1' Permeability of porous medium	Gr Thermal Grashof number
Pr Prandtl number	a Absorption constant
M Magnetic parameter	q_r Radiative heat flux
Sr Soret effect parameter	T' Fluid temperature

u' Fluid velocity in g direction

t' Time

t Dimensionless time

Sc Schmidt Number

Greek symbols:

$\emptyset$ porosity of the fluid

β'_T Volumetric coefficient of thermal expansion

β'_c Volumetric coefficient of species concentration expansion

$\mu\beta$ plastic dynamic viscosity,

ν Kinematic viscosity coefficient

ρ Fluid density

σ Electrical conductivity

γ Casson parameter

1. Introduction:

Magnetohydrodynamics flow of a Non-Newtonian fluid is a part of fluid mechanics. It is based on the principle that fluid particles may be considered as continuous in a structure. Pseudo plastic time independent fluid is one of the non-newtonian fluids in which viscosity decreases with increasing velocity gradient e.g. polymer solutions, blood etc. Casson fluid is one of the Pseudo plastic fluids. It means that it is Shear thinning fluid. The fluid is more viscous as compare to Newtonian fluids at low shear rates and is less viscous when shear rate is high.

Casson [1] introduced Casson fluid model for the prediction of the flow behavior of pigment-oil suspensions. Today MHD has advanced into a huge field of practical and fundamental research in engineering and physical science. First exact solution of MHD equations was found by Hartmann [2]. Kataria and Mittal [3] - [4], considered free convective nanofluid flow with heat transfer problems. The radiations due to heat transfer effects on different flows are very important in space technology and high temperature processes. Kataria et al. [6] considered magnetic field effects on micro-polar fluid between two vertical walls. Unsteady free convective MHD flow with heat and mass transfer is important in engineering and technology. Thermal radiation parameter effects may play an important role in controlling heat transfer in polymer processing industry. Some of the vital applications of heat and mass transfer flow with chemical reaction can be found in catalytic chemical reactors, food processing and polymer production. Research studies related to heat generating or heat absorbing fluid flow is of considerable importance in several physical problems. Kataria and Patel [7] - [8] considered unsteady free convective MHD flow with ramped wall temperature. Recently, Kataria and Patel [9] obtained the solution of radiation and reaction effects MHD Casson fluid flow past an oscillating vertical plate in embedded porous medium. Such effects are important when thickness changes happen in the flow regime. For example, when species are introduced at surface in fluid domain, with different (lower) density compared to the surrounding fluid, Soret effects can be significant. Some of relevant research studies are due to Kataria and Patel [10].

Purpose of this paper is to investigate exact solution of radiative and parabolic motion effects on unsteady free convective MHD flow of Casson fluid past over vertical plate embedded in porous medium in a rotating system with ramped wall temperature. Such study may find application in fire dynamics in insulations and geothermal energy systems etc.

2. Mathematical formulation of the problem

In Figure 1 the flow being confined to $y' > 0$, where y' the coordinate is measured in the normal direction to the plate and $x' -$ axis is taken along the wall in the upward direction. Initially, at time $t' = 0$, both the fluid and the plate are uniform temperature T'_∞ and the concentration near the plate is assumed to be C'_∞ at all the points respectively. At time $t' > 0$, the flow being parabolic motion in the vertical direction against gravitational field with velocity $U_0 t'^2$ and constant heat flux, $T'_\infty + (T'_w + T'_\infty)\, t'/t_0$ when $t' \le t_0$ and T'_w when $t' > t_0$ respectively which is there after maintained constant T'_w and the level of mass transfer at the surface of the plate is raised or lowered to $C'_\infty + (C'_w + C'_\infty)\, t'/t_0$ when $t' \le t_0$ and C'_w when $t' > t_0$ respectively which is there after maintained constant C'_w. A uniformly magnetic field of strength B_0 is applied in the $y' -$ axis direction. Under these condition we get the following partial differential equation with initial and boundary condition are given below.

$$\rho \frac{\partial u'}{\partial t'} = \mu_B \left(1 + \frac{1}{\gamma}\right) \frac{\partial^2 u'}{\partial y^2} - \sigma B_0^2 u' - \frac{\mu \emptyset}{k_1'} u' + \rho g \beta'_T (T' - T'_\infty) + \rho g \beta'_C (C' - C'_\infty) \quad (1)$$

$$\frac{\partial T'}{\partial t'} = \frac{k}{\rho c_p} \frac{\partial^2 T'}{\partial y'^2} - \frac{1}{\rho c_p} \frac{\partial q_r}{\partial y'} \quad (2)$$

$$\frac{\partial C'}{\partial t'} = D_M \frac{\partial^2 C'}{\partial y'^2} - D_T (T' - T'_\infty) + k_2' (C' - C'_\infty) \quad (3)$$

With following initial and boundary conditions:

$$u' = 0,\ T' = T'_\infty,\ C' = C'_\infty;\ as\ \ y' \ge 0\ and\ \ t' \le 0,\ u' = U_0 t'^2,\ \ as\ \ t' > 0\ and\ y' = 0\ ,$$

$$T' = \begin{cases} T'_\infty + (T'_w - T'_\infty)\, t'/t_0\ if\ \ 0 < t' < t_0 \\ T'_w \qquad\qquad if \quad t' \ge t_0 \end{cases}, C' = \begin{cases} C'_\infty + (C'_w - C'_\infty)\, t'/t_0\ if\ \ 0 < t' < t_0 \\ C'_w \qquad\qquad if \quad t' \ge t_0 \end{cases};$$

$$y' = 0$$

$$u' \to 0, T' \to T'_\infty,\ \ C' \to C'_\infty;\ as\ \ y' \to \infty\ and\ t' \ge 0 \quad (4)$$

As we have optically thick Casson fluid, we can use Rosseland approximation [11]

$$\frac{\partial q_r}{\partial y'} = -4a\sigma (T'^4_\infty - T'^4) \quad (5)$$

Where a is absorption constant

T'^4 can be expand as the linear temperature function. Using Taylor series expanding T'^4 about T'_∞ and higher order term are neglecting.

$$T'^4 \cong 4T'^3_\infty T' - 3T'^4_\infty \quad (6)$$

Where

$$y = \frac{y'}{U_0 t_0},\ u = \frac{u'}{U_0},\ t = \frac{t'}{t_0},\ \theta = \frac{(T' - T'_\infty)}{(T'_w - T'_\infty)},\ C = \frac{(C' - C'_\infty)}{(C'_w - C'_\infty)},\ Gr = \frac{\nu g \beta'_T (T'_w - T'_\infty)}{U_0^3}$$

$$Gm = \frac{\nu g \beta'_C (C'_w - C'_\infty)}{U_0^3},\ M = \frac{\sigma B_0^2 \nu}{\rho U_0^2},\ P_r = \frac{\rho \nu C_p}{k}, R = \frac{16\, a\, \sigma \nu^2 T'^3_\infty}{k\, U_0^2},\ Sc = \frac{\nu}{D_M}$$

Input (5) and (6) in (3) and in the equations (1-3) dropping out the " ′ " notation (for simplicity) we get

$$\frac{\partial u}{\partial t} = \left(1 + \frac{1}{\gamma}\right) \frac{\partial^2 u}{\partial y^2} - \left(M^2 + \frac{1}{k}\right) u + G_r \theta + G_m C \quad (7)$$

$$\frac{\partial \theta}{\partial t} = \frac{1}{Pr}\frac{\partial^2 \theta}{\partial y^2} - \frac{R}{Pr}\theta \tag{8}$$

$$\frac{\partial C}{\partial t} = \frac{1}{s_c}\frac{\partial^2 C}{\partial y^2} - Krc + Sr\theta \tag{9}$$

With initial and boundary condition

$u = \theta = C = 0\,, \qquad y \geq 0, t \leq 0$

$u = t^2\,,\ \theta = \begin{cases} t, & 0 < t \leq 1 \\ 1 & t > 1 \end{cases} = tH(t) - (t-1)H(t-1)$

$C = \begin{cases} t, & 0 < t \leq 1 \\ 1 & t > 1 \end{cases} = tH(t) - (t-1)H(t-1) \qquad at\ \ y = 0,\ t > 0$

$u \to 0, \theta \to 0, C \to 0 \quad at\ \ y \to \infty$ (10)

Where

H (.) is Heaviside unit step function.

Solution:

Case I: For ramped wall temperature and ramped surface concentration.

Taking Laplace transform to equations (7), (8) and (9) with initial conditions and boundary conditions of equation (10)

$$\bar{\theta} = (1 - e^{-s})F_7(y, s) \tag{11}$$

$$\bar{C} = (1 - e^{-s})F_{11}(y, s) - (1 - e^{-s})G_9(y, s) + (1 - e^{-s})G_{10}(y, s) \tag{12}$$

$$\bar{u} = G_1(y, s) + (1 - e^{-s})H_1(y, s) \tag{13}$$

Case II: For constant temperature and ramped surface concentration.

In this case, the initial and boundary conditions are the same excluding Eq. (10) that becomes $\theta = 1\ at\ y = 0, t \geq 0$ .We find the isothermal temperature $\theta(y, t)$ using Laplace transform

$$\bar{\theta} = F_6(y, s) \tag{14}$$

$$\bar{C} = (1 - e^{-s})F_{11}(y, s) - a_{54}F_{10}(y, s) + a_{54}F_{13}(y, s) + a_{54}F_6(y, s) - a_{54}F_9(y, s) \tag{15}$$

$$\begin{aligned}\bar{u} = {} & G_1(y, s) + a_{49}F_1(y, s) + a_{50}F_3(y, s) + a_{51}F_5(y, s) + a_{46}F_4(y, s) + (1 - e^{-s})G_5(y, s) \\ & + a_{40}F_6(y, s) - a_{50}F_8(y, s) + a_{47}F_9(y, s) + a_{26}F_{10}(y, s) + a_{45}F_{13}(y, s) + a_{46}F_{12}(y, s) \\ & - G_6(y, s)(1 - e^{-s})\end{aligned} \tag{16}$$

Case III: For ramped wall temperature and constant surface concentration.

In this case, the initial and boundary conditions are the same excluding Eq. (10) that becomes $C = 1\ at\ y = 0, t \geq 0$ .We find the constant surface concentration $C(y, t)$ using Laplace transform

$$\bar{\theta} = (1 - e^{-s})F_7(y, s) \tag{17}$$

$$\bar{C} = F_{10}(y, s) - (1 - e^{-s})G_9(y, s) + (1 - e^{-s})G_{10}(y, s) \tag{18}$$

$$\begin{aligned}\bar{u} = {} & G_1(y, s) + (1 - e^{-s})G_7(y, s) + a_{23}F_1(y, s) - a_{23}F_4(y, s) + (1 - e^{-s})G_3(y, s) \\ & + (1 - e^{-s})G_8(y, s) - a_{23}F_{10}(y, s) + a_{23}F_{11}(y, s)\end{aligned} \tag{19}$$

Case IV: For constant temperature and constant surface concentration.

In this case, the initial and boundary conditions are the same excluding Eq. (10) that becomes $\theta = 1 \; and \; C = 1 \; at \; y = 0, t \geq 0$ .We find the isothermal temperature $\theta(y,t)$ and constant surface concentration C(y , t) using Laplace transform

$$\bar{\theta} = F_6(y,s) \tag{20}$$

$$\bar{C} = F_{10}(y,s) - a_{54}F_{10}(y,s) + a_{54}F_{13}(y,s) + a_{54}F_6(y,s) - a_{54}F_9(y,s) \tag{21}$$

$$\bar{u} = G_1(y,s) + a_{35}F_1(y,s) + a_{50}F_3(y,s) - a_{53}F_4(y,s) + a_{51}F_5(y,s) + a_{40}F_6(y,s) - a_{50}F_8(y,s) - a_{47}F_9(y,s) + a_{43}F_{10}(y,s) + a_{53}F_{12}(y,s) + a_{45}F_{13}(y,s) \tag{22}$$

Where

$$H_1(y,s) = G_2(y,s) + G_3(y,s) + G_4(y,s) \tag{23}$$

$$G_1(y,s) = \frac{2}{s^3}e^{-\sqrt{\frac{s+b}{a}}} \tag{24}$$

$$G_2(y,s) = a_{34}F_1(y,s) + a_{35}F_2(y,s) + a_{36}F_3(y,s) + a_{37}F_4(y,s) + a_{38}F_5(y,s) \tag{25}$$

$$G_3(y,s) = a_{39}F_6(y,s) + a_{40}F_7(y,s) + a_{41}F_8(y,s) - a_{32}F_9(y,s) \tag{26}$$

$$G_4(y,s) = a_{42}F_{10}(y,s) + a_{43}F_{11}(y,s) + a_{44}F_{12}(y,s) + a_{28}F_{13}(y,s) \tag{27}$$

$$G_5(y,s) = a_{25}F_1(y,s) + a_{23}F_2(y,s) + a_{24}F_4(y,s) \tag{28}$$

$$G_6(y,s) = a_{25}F_{10}(y,s) + a_{23}F_{11}(y,s) + a_{24}F_{12}(y,s) \tag{29}$$

$$G_7(y,s) = a_{52}F_1(y,s) + a_{49}F_2(y,s) + a_{36}F_3(y,s) + a_7F_4(y,s) + a_{38}F_5(y,s) \tag{30}$$

$$G_8(y,s) = a_{29}F_{10}(y,s) + a_{26}F_{11}(y,s) + a_{27}F_{12}(y,s) + a_{28}F_{13}(y,s) \tag{31}$$

$$G_9(y,s) = a_{56}F_{10}(y,s) + a_{54}F_{11}(y,s) + a_{55}F_{13}(y,s) \tag{32}$$

$$G_{10}(y,s) = a_{56}F_6(y,s) + a_{57}F_7(y,s) + a_{35}F_9(y,s) \tag{33}$$

$$F_1(y,s) = \frac{1}{s}e^{-y\sqrt{\frac{s+b}{a}}} \tag{34}$$

$$F_2(y,s) = \frac{1}{s^2}e^{-y\sqrt{\frac{s+b}{a}}} \tag{35}$$

$$F_3(y,s) = \frac{1}{(s+a_{12})}e^{-y\sqrt{\frac{s+b}{a}}} \tag{36}$$

$$F_4(y,s) = \frac{1}{(s+a_{16})}e^{-y\sqrt{\frac{s+b}{a}}} \tag{37}$$

$$F_5(y,s) = \frac{1}{(s+a_6)}e^{-y\sqrt{\frac{s+b}{a}}} \tag{38}$$

$$F_6(y,s) = \frac{1}{s}e^{-y\sqrt{R+\,p_r\,s}} \tag{39}$$

$$F_7(y,s) = \frac{1}{s^2}e^{-y\sqrt{R+\,p_r\,s}} \tag{40}$$

$$F_8(y,s) = \frac{1}{(s+a_{12})}e^{-y\sqrt{R+\,p_r\,s}} \tag{41}$$

$$F_9(y,s) = \frac{1}{(s+a_6)}e^{-y\sqrt{R+\,p_r\,s}} \tag{42}$$

$$F_{10}(y,s) = \frac{1}{s}e^{-y\sqrt{s_c\,s+a_2)}} \tag{43}$$

$$F_{11}(y,s) = \frac{1}{s^2}e^{-y\sqrt{s_c\,s+a_2)}} \tag{44}$$

$$F_{12}(y,s) = \frac{1}{(s+a_{16})}e^{-y\sqrt{s_c\,s+a_2)}} \tag{45}$$

$$F_{13}(y,s) = \frac{1}{(s+a_6)} e^{-y\sqrt{s_c\, s+a_2)}} \tag{46}$$

Taking Inverse Laplace transform from equation (11) to (46)

Case I: For ramped wall temperature and ramped surface concentration.

$$\theta(y,t) = f_7(y,t) - H(t-1)f_7(y,t-1) \tag{47}$$

$$C(y,t) = f_{11}(y,t) - H(t-1)f_{11}(y,t-1) - g_9(y,t) + H(t-1)g_9(y,t-1) + g_{10}(y,t) - H(t-1)g_{10}(y,t-1) \tag{48}$$

$$u(y,t) = g_1(y,t) + h_1(y,t) - H(y,t-1)h_1(y,t) \tag{49}$$

Case II: For constant temperature and ramped surface concentration.

$$\theta(y,t) = f_6(y,t) \tag{50}$$

$$C(y,t) = f_{11}(y,t) - H(t-1)f_{11}(y,t-1) - a_{54}f_{10}(y,t) + a_{54}f_{13}(y,t) + a_{54}f_6(y,t) - a_{54}f_9(y,t) \tag{51}$$

$$u(y,t) = g_1(y,t) + a_{49}f_1(y,t) + a_{50}f_3(y,t) + a_{51}f_5(y,t) + a_{46}f_4(y,t) + g_5(y,t) - H(t-1)g_5(y,t-1) + a_{40}f_6(y,t) - a_{50}f_8(y,t) + a_{47}f_9(y,t) + a_{26}f_{10}(y,t) + a_{45}f_{13}(y,t) + a_{46}f_{12}(y,t) - g_6(y,t) - g_6(y,t-1)H(t-1) \tag{52}$$

Case III: For ramped wall temperature and constant surface concentration.

$$\theta(y,t) = f_7(y,t) - f_7(y,t-1)H(t-1) \tag{53}$$

$$C(y,t) = f_{10}(y,t) - g_9(y,t) + g_9(y,t-1)H(t-1) + g_{10}(y,t) - g_{10}(y,t-1)H(t-1) \tag{54}$$

$$u(y,t) = g_1(y,t) + g_7(y,t) - g_7(y,t-1)H(t-1) + a_{23}f_1(y,t) - a_{23}f_4(y,t) + g_3(y,t) - g_3(y,t-1)H(t-1) + g_8(y,t) - g_8(y,t-1)H(t-1) - a_{23}f_{10}(y,t) + a_{23}f_{11}(y,t) \tag{55}$$

Case IV: For constant temperature and constant surface concentration.

$$\theta(y,t) = f_6(y,t) \tag{56}$$

$$C(y,t) = f_{10}(y,t) - a_{54}f_{10}(y,t) + a_{54}f_{13}(y,t) + a_{54}f_6(y,t) - a_{54}f_9(y,t) \tag{57}$$

$$u(y,t) = g_1(y,t) + a_{35}f_1(y,t) + a_{50}f_3(y,t) - a_{53}f_4(y,t) + a_{51}f_5(y,t) + a_{40}f_6(y,t) - a_{50}f_8(y,t) - a_{47}f_9(y,t) + a_{43}f_{10}(y,t) + a_{53}f_{12}(y,t) + a_{45}f_{13}(y,t) \tag{58}$$

Where

$$h_1(y,t) = g_2(y,t) + g_3(y,t) + g_4(y,t) \tag{59}$$

$$g_2(y,t) = a_{34}f_1(y,t) + a_{35}f_2(y,t) + a_{36}f_3(y,t) + a_{37}f_4(y,t) + a_{38}f_5(y,t) \tag{60}$$

$$g_3(y,t) = a_{39}f_6(y,t) + a_{40}f_7(y,t) + a_{41}f_8(y,t) - a_{32}f_9(y,t) \tag{61}$$

$$g_4(y,t) = a_{42}f_{10}(y,t) + a_{43}f_{11}(y,t) + a_{44}f_{12}(y,t) + a_{28}f_{13}(y,t) \tag{62}$$

$$g_5(y,t) = a_{25}f_1(y,t) + a_{23}f_2(y,t) + a_{24}f_4(y,t) \tag{63}$$

$$g_6(y,t) = a_{25}f_{10}(y,t) + a_{23}f_{11}(y,t) + a_{24}f_{12}(y,t) \tag{64}$$

$$g_7(y,t) = a_{52}f_1(y,t) + a_{49}f_2(y,t) + a_{36}f_3(y,t) + a_7f_4(y,t) + a_{38}f_5(y,t) \tag{65}$$

$$g_8(y,t) = a_{29}f_{10}(y,t) + a_{26}f_{11}(y,t) + a_{27}f_{12}(y,t) + a_{28}f_{13}(y,t) \tag{66}$$

$$g_9(y,t) = a_{56}f_{10}(y,t) + a_{54}f_{11}(y,t) + a_{55}f_{13}(y,t) \tag{67}$$

$$g_{10}(y,t) = a_{56}f_6(y,t) + a_{57}f_7(y,t) + a_{35}f_9(y,t) \tag{68}$$

$$g_1(y,t) = \int_0^t f_1(y,u)\,2(t-u)du \tag{69}$$

$$f_1(y,t) = \frac{1}{2}\left[e^{-y\sqrt{\frac{b}{a}}}\,erfc\,\left(\frac{y}{2\sqrt{at}} - \sqrt{bt}\right) + e^{y\sqrt{\frac{b}{a}}}\,erfc\,\left(\frac{y}{2\sqrt{at}} + \sqrt{bt}\right)\right] \tag{70}$$

$$f_2(y,t) = \frac{1}{2}\left[\left(t - \frac{y}{2\sqrt{ab}}\right)e^{-y\sqrt{\frac{b}{a}}}\,erfc\,\left(\frac{y}{2\sqrt{at}} - \sqrt{bt}\right) + \left(t + \frac{y}{2\sqrt{ab}}\right)e^{y\sqrt{\frac{b}{a}}}\,erfc\,\left(\frac{y}{2\sqrt{at}} + \sqrt{bt}\right)\right] \tag{71}$$

$$f_3(y,t) = \frac{e^{-a_{12}t}}{2}\left[e^{-y\sqrt{\frac{1}{a}(b-a_{12})}}\,erfc\,\left(\frac{y}{2\sqrt{a\,t}} - \sqrt{(b-a_{12})t}\right) + e^{y\sqrt{\frac{1}{a}(b-a_{12})}}\,erfc\,\left(\frac{y}{2\sqrt{a\,t}} + \sqrt{(b-a_{12})t}\right)\right] \tag{72}$$

$$f_4(y,t) = \frac{e^{-a_{16}t}}{2}\left[e^{-y\sqrt{\frac{1}{a}(b-a_{16})}}\,erfc\,\left(\frac{y}{2\sqrt{a\,t}} - \sqrt{(b-a_{16})t}\right) + e^{y\sqrt{\frac{1}{a}(b-a_{16})}}\,erfc\,\left(\frac{y}{2\sqrt{a\,t}} + \sqrt{(b-a_{16})t}\right)\right] \tag{73}$$

$$f_5(y,t) = \frac{e^{-a_6t}}{2}\left[e^{-y\sqrt{\frac{1}{a}(b-a_6)}}\,erfc\,\left(\frac{y}{2\sqrt{a\,t}} - \sqrt{(b-a_6)t}\right) + e^{y\sqrt{\frac{1}{a}(b-a_6)}}\,erfc\,\left(\frac{y}{2\sqrt{a\,t}} + \sqrt{(b-a_6)t}\right)\right] \tag{74}$$

$$f_6(y,t) = \frac{1}{2}\left[e^{-y\sqrt{R}}\,erfc\,\left(\frac{y\sqrt{Pr}}{2\sqrt{t}} - \sqrt{\frac{R}{Pr}t}\right) + e^{y\sqrt{R}}\,erfc\,\left(\frac{y\sqrt{Pr}}{2\sqrt{t}} + \sqrt{\frac{R}{Pr}t}\right)\right] \tag{75}$$

$$f_7(y,t) = \frac{1}{2}\left[\left(t - \frac{y\,Pr}{2\sqrt{R}}\right)e^{-y\sqrt{R}}\,erfc\,\left(\frac{y\sqrt{Pr}}{2\sqrt{t}} - \sqrt{\frac{R}{Pr}t}\right) + \left(t + \frac{y\,Pr}{2\sqrt{R}}\right)e^{y\sqrt{R}}\,erfc\,\left(\frac{y\sqrt{Pr}}{2\sqrt{t}} + \sqrt{\frac{R}{Pr}t}\right)\right] \tag{76}$$

$$f_8(y,t) = \frac{e^{-a_{12}t}}{2}\left[e^{-y\sqrt{R-Pr\,a_{12}}}\,erfc\,\left(\frac{y\sqrt{Pr}}{2\sqrt{t}} - \sqrt{\left(\frac{R}{Pr} - a_{12}\right)t}\right) + e^{y\sqrt{R-Pr\,a_{12}}}\,erfc\,\left(\frac{y\sqrt{Pr}}{2\sqrt{t}} + \sqrt{\left(\frac{R}{Pr} - a_{12}\right)t}\right)\right] \tag{77}$$

$$f_9(y,t) = \frac{e^{-a_6t}}{2}\left[e^{-y\sqrt{R-Pr\,a_6}}\,erfc\,\left(\frac{y\sqrt{Pr}}{2\sqrt{t}} - \sqrt{\left(\frac{R}{Pr} - a_6\right)t}\right) + e^{y\sqrt{R-Pr\,a_6}}\,erfc\,\left(\frac{y\sqrt{Pr}}{2\sqrt{t}} + \sqrt{\left(\frac{R}{Pr} - a_6\right)t}\right)\right] \tag{78}$$

$$f_{10}(y,t) = \frac{1}{2}\left[e^{-y\sqrt{a_2}}\,erfc\,\left(\frac{y\sqrt{Sc}}{2\sqrt{t}} - \sqrt{\frac{a_2}{Sc}t}\right) + e^{y\sqrt{a_2}}\,erfc\,\left(\frac{y\sqrt{Sc}}{2\sqrt{t}} + \sqrt{\frac{a_2}{Sc}t}\right)\right] \tag{79}$$

$$f_{11}(y,t) = \frac{1}{2}\left[\left(t - \frac{y\,Sc}{2\sqrt{a_2}}\right)e^{-y\sqrt{a_2}}\,erfc\,\left(\frac{y\sqrt{Sc}}{2\sqrt{t}} - \sqrt{\frac{a_2}{Sc}t}\right) + \left(t + \frac{y\,Sc}{2\sqrt{a_2}}\right)e^{y\sqrt{a_2}}\,erfc\,\left(\frac{y\sqrt{Sc}}{2\sqrt{t}} + \sqrt{\frac{a_2}{Sc}t}\right)\right] \tag{80}$$

$$f_{12}(y,t) = \frac{e^{-a_{16}t}}{2}\left[e^{-y\sqrt{a_2-Sc\,a_{16}}}\,erfc\,\left(\frac{y\sqrt{Sc}}{2\sqrt{t}} - \sqrt{\left(\frac{a_2}{Sc} - a_{16}\right)t}\right) + e^{y\sqrt{a_2-Sc\,a_{16}}}\,erfc\,\left(\frac{y\sqrt{Sc}}{2\sqrt{t}} + \sqrt{\left(\frac{a_2}{Sc} - a_{16}\right)t}\right)\right] \tag{81}$$

$$f_{13}(y,t) = \frac{e^{-a_6t}}{2}\left[e^{-y\sqrt{a_2-Sc\,a_6}}\,erfc\,\left(\frac{y\sqrt{Sc}}{2\sqrt{t}} - \sqrt{\left(\frac{a_2}{Sc} - a_6\right)t}\right) + e^{y\sqrt{a_2-Sc\,a_6}}\,erfc\,\left(\frac{y\sqrt{Sc}}{2\sqrt{t}} + \sqrt{\left(\frac{a_2}{Sc} - a_6\right)t}\right)\right] \tag{82}$$

3. Result and discussion

Effects of magnetic field M, Casson fluid parameter γ, permeability of porous medium k, thermal radiation R, Chemical reaction Kr and Sorret effect Sr on velocity, temperature and concentration profiles are shown for all thermal and concentration 4 possibilities of boundary conditions through various graphical figures.

As magnetic field parameter M increases, velocity decreases due to Lorentz force which is reflected in Figure 2. Figure 3 describes that raise of Casson fluid parameter γ also decreases velocity. If we increase Permeability of porous medium, then flow should be faster means velocity should increase which is observed in figure 4.

Figures 5 and 6 shows that velocity and temperatures both decrease on increment of thermal radiation R. Physically, when the amount of heat generated through thermal radiation parameter increases, the bond holding the components of the fluid particles is easily broken and the fluid velocity will increase. The effect of increment in chemical reaction Kr also decreases velocity and concentration due to buoyancy effect which are described in figures 7 and 8. Whereas growth of Soret effect Sr gives positive impacts on velocity and concentration as observed in figures 9 and 10. Grashoff number Gr and mass Grashoff number Gm have affirmative relation with velocity which can be seen in figures 11 and 12 respectively.

Conclusion

The most important concluding remarks can be summarized as follows:

- Casson fluid parameter γ, permeability of porous medium k, Soret effect Sr, Grashoff number Gr and mass Grashoff number Gm have positive impacts with velocity.
- Magnetic field parameter M, Thermal radiation R and chemical reaction Kr have retarding effects with velocity.
- Thermal radiation parameter R have negative impact on temperature.
- Concentration of the fluid decreases if Chemical reaction parameter Kr value is increased but it increases if Soret effect Sr value is raised.

Appendix:

$$a = 1 + \frac{1}{\gamma} \qquad b = M^2 + \frac{1}{k} \qquad a_1 = R' - sr$$

$$a_2 = Sc\ a_1 \qquad a_3 = Kr.Sc \qquad a_4 = R - a_2$$

$$a_5 = Pr - Sc \qquad a_6 = \frac{a_4}{a_5} \qquad a_7 = \frac{a_3}{a_5}$$

$$a_8 = \frac{Gr}{a} \qquad a_9 = \frac{Gm}{a} \qquad a_{10} = R - \frac{b}{a}$$

$$a_{11} = Pr - \frac{1}{a} \qquad a_{12} = \frac{a_{10}}{a_{11}} \qquad a_{13} = \frac{a_8}{a_{11}}$$

$$a_{14} = a_2 - \frac{b}{a} \qquad a_{15} = Sc - \frac{1}{a} \qquad a_{16} = \frac{a_{14}}{a_{15}}$$

$$a_{17} = \frac{a_9}{a_{15}} \qquad a_{18} = \frac{a_9\ a_7}{a_{15}} \qquad a_{19} = \frac{a_9\ a_7}{a_{11}}$$

$$a_{20} = \frac{a_{13}}{a_{12}} \qquad a_{21} = \frac{a_{13}}{{a_{12}}^2} \qquad a_{22} = \frac{a_{13}}{(1+a_{12})} - a_{20} - \frac{a_{21}}{(1+a_{12})}$$

$$a_{23} = \frac{a_{17}}{a_{16}} \qquad a_{24} = \frac{a_{17}}{{a_{16}}^2} \qquad a_{25} = \frac{a_{17}}{(1+a_{16})} - a_{23} - \frac{a_{24}}{(1+a_{16})}$$

$$a_{26} = \frac{a_{18}}{a_6\ a_{16}} \qquad a_{27} = \frac{a_{18}}{{a_{16}}^2(a_6 - a_{16})} \qquad a_{28} = \frac{a_{18}}{{a_6}^2(a_{16} - a_6)}$$

$$a_{30} = \frac{a_{19}}{a_6\ a_{12}} \qquad a_{31} = \frac{a_{19}}{{a_{12}}^2(a_6 - a_{12})} \qquad a_{29} = \frac{a_{18}}{(1+a_6)\,(1+a_{16})} - a_{26} - \frac{a_{27}}{(1+a_{16})} - \frac{a_{28}}{(1+a_6)}$$

$$a_{32} = \frac{a_{19}}{{a_6}^2(a_{12} - a_6)} \qquad a_{34} = a_{22} + a_{25} - a_{29} + a_{33} \qquad a_{33} = \frac{a_{19}}{(1+a_6)\,(1+a_{12})} - a_{30} - \frac{a_{31}}{(1+a_{12})} - \frac{a_{32}}{(1+a_6)}$$

$$a_{35} = a_{20} + a_{23} - a_{26} + a_{30} \qquad a_{36} = a_{21} + a_{31} \qquad a_{37} = a_{24} - a_{27}$$

$$a_{38} = -a_{28} + a_{32} \qquad a_{39} = -a_{22} - a_{33} \qquad a_{40} = -a_{20} - a_{30}$$

$$a_{41} = -a_{21} - a_{31} \qquad a_{42} = -a_{25} + a_{29} \qquad a_{43} = -a_{23} + a_{26}$$

$$a_{44} = -a_{24} + a_{27} \qquad a_{45} = -\frac{a_{18}}{a_6(a_{16} - a_6)} \qquad a_{46} = -\frac{a_{18}}{a_{16}(a_6 - a_{16})}$$

$a_{47} = -\frac{a_{19}}{a_6(a_{12}-a_6)}$ $a_{48} = -\frac{a_{18}}{a_{12}(a_6-a_{12})}$ $a_{49} = a_{20} - a_{26} + a_{30}$

$a_{50} = a_{48} - a_{20}$ $a_{51} = -a_{45} + a_{47}$ $a_{52} = a_{22} - a_{29} + a_{33}$

$a_{53} = -a_{23} - a_{46}$ $a_{54} = \frac{a_7}{a_6}$ $a_{56} = \frac{a_7}{(1+a_6)} - a_{54} - \frac{a_{55}}{(1+a_6)}$

$a_{55} = \frac{a_7}{a_6{}^2}$

References

[1] Casson, N., (1959): A flow equation for the pigment oil suspensions of the printing ink type, in: Rheology of Disperse Systems, Pergamon, NewYork, 84-102.

[2] Hartmann, J., (1937): Hg-dynamics I theory of the laminar flow of an electrically conductive liquid in a homogenous magnetic field, Det Kal. Danske Videnskabernes selskab, Mathematisk-fysiske Meddeleser, 15 1-27.

[3] Kataria, H. R., Mittal, A. S., (2015): Mathematical model for velocity and temperature of gravity-driven convective optically thick nanofluid flow past an oscillating vertical plate in presence of magnetic field and radiation. Journal of Nigerian Mathematical Society, 34 303–317.

[4] Kataria, H. R., Mittal, A. S., (2017): Velocity, mass and temperature analysis of gravity-driven convection nanofluid flow past an oscillating vertical plate in presence of magnetic field in a porous medium, Applied Thermal Engineering, 110 864-874.

[5] Kataria, H. R., Mittal, A. S., (2017): Analysis of Casson nanofluid flow in presence of magnetic field and radiation, Mathematics Today, 33(1), 99 - 120.

[6] Kataria, H. R., Patel, H. R., (2015): Effect of magnetic field on unsteady natural convective flow of a micropolar fluid between two vertical walls, Ain Shams Engineering Journal, doi. 10.1016/j.asej.2015.08.013.

[7] Kataria, H. R., Patel, H. R., (2016): Heat and Mass Transfer in MHD Second Grade Fluid Flow with Ramped Wall Temperature through Porous Medium, Mathematics Today, 32 67-83

[8] Kataria, H. R., Patel, H. R., (2016): Effect of thermo-diffusion and parabolic motion on MHD Second grade fluid flow with ramped wall temperature and ramped surface concentration, Alexandria Engineering Journal, 10.1016/j.aej.2016.11.014

[9] Kataria, H. R., Patel, H. R., (2016): Radiation and chemical reaction effects on MHD Casson fluid flow past an oscillating vertical plate embedded in porous medium, Alexandria Engineering Journal, 55 583–595

[10] Kataria, H. R., Patel, H. R., (2016): soret and heat generation effects on MHD Casson fluid flow past an oscillating vertical plate embedded through porous medium, Alexandria Engineering Journal 55 2125–2137

[11] Rosseland, S., (1931): Astrophysik und atom-theoretische Grundlagen. Berlin: Springer-Verlag.

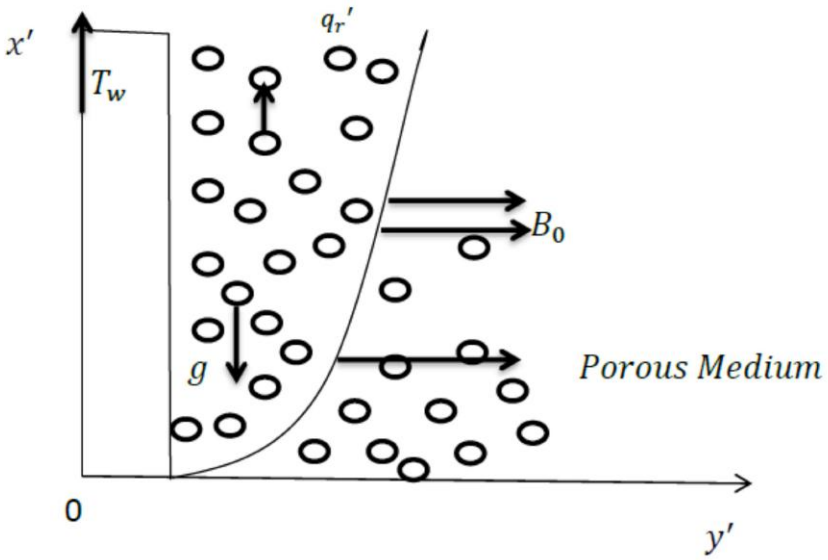

Figure 1: Physical sketch of the problem

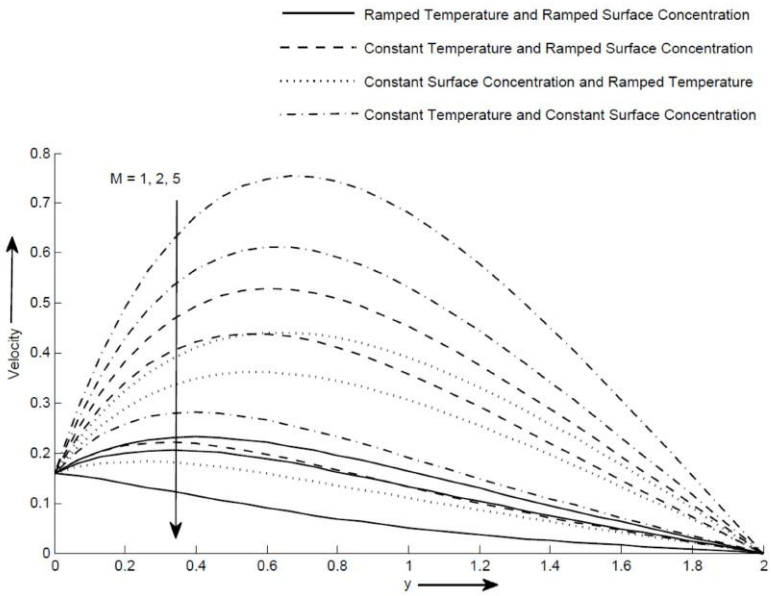

Figure 2: Velocity profile for different values of M and y

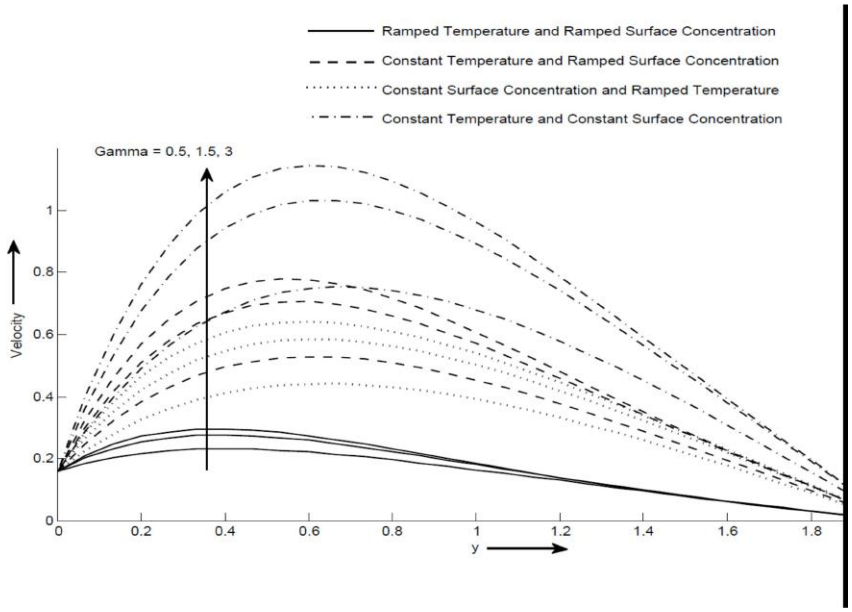

Figure 3: Velocity profile for different values of γ and y

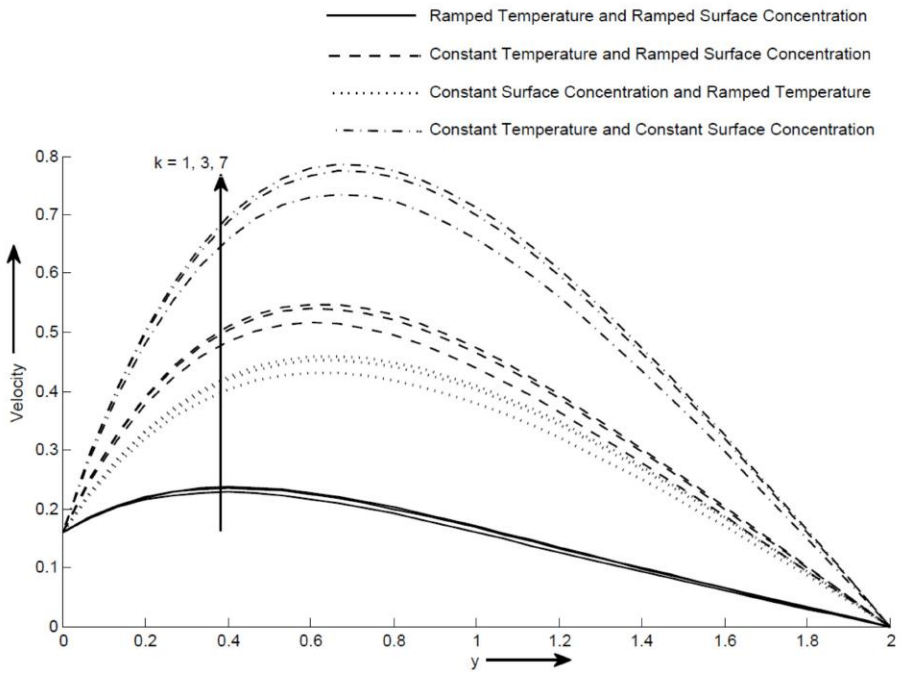

Figure 4: Velocity profile for different values of K and y

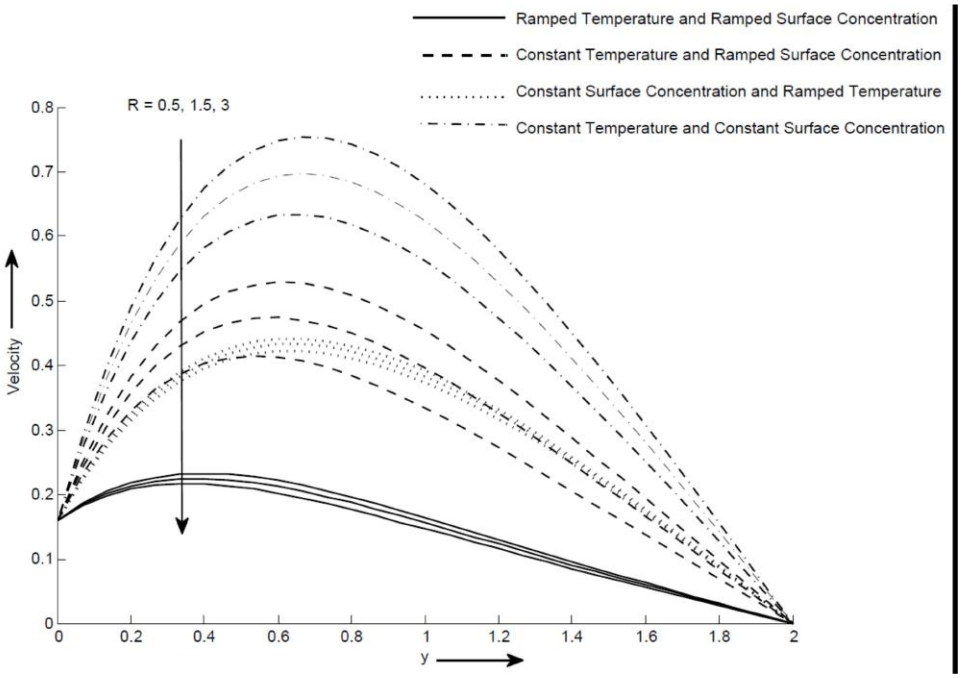

Figure 5: Velocity profile for different values of R and y

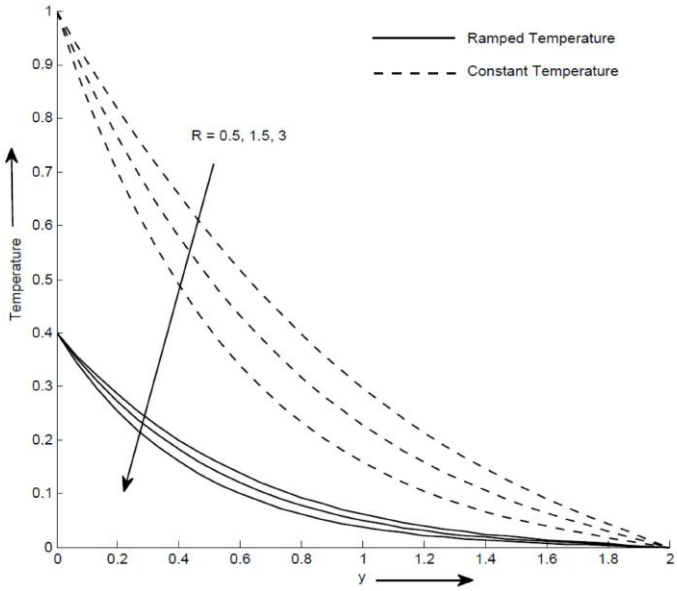

Figure 6: Temperature profile for different values of R and y

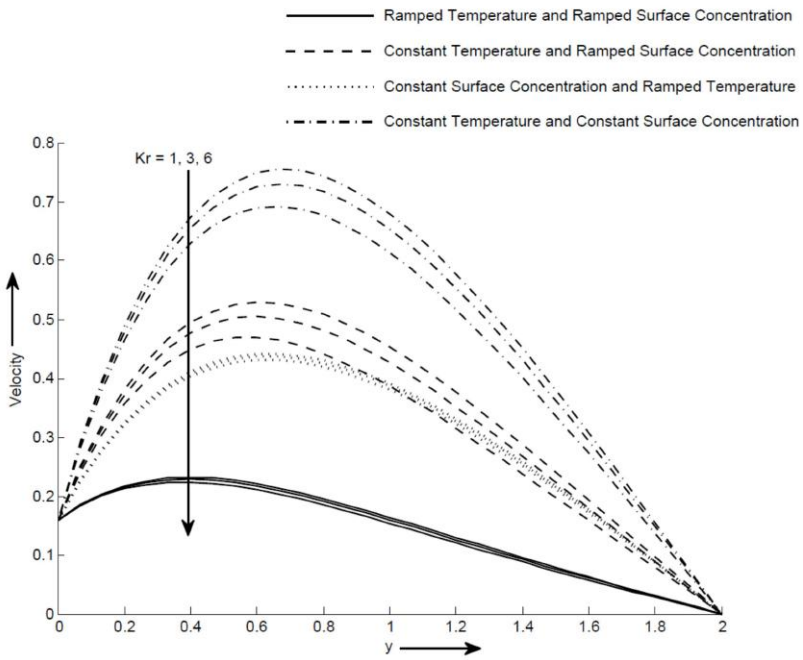

Figure 7: Velocity profile for different values of Kr and y

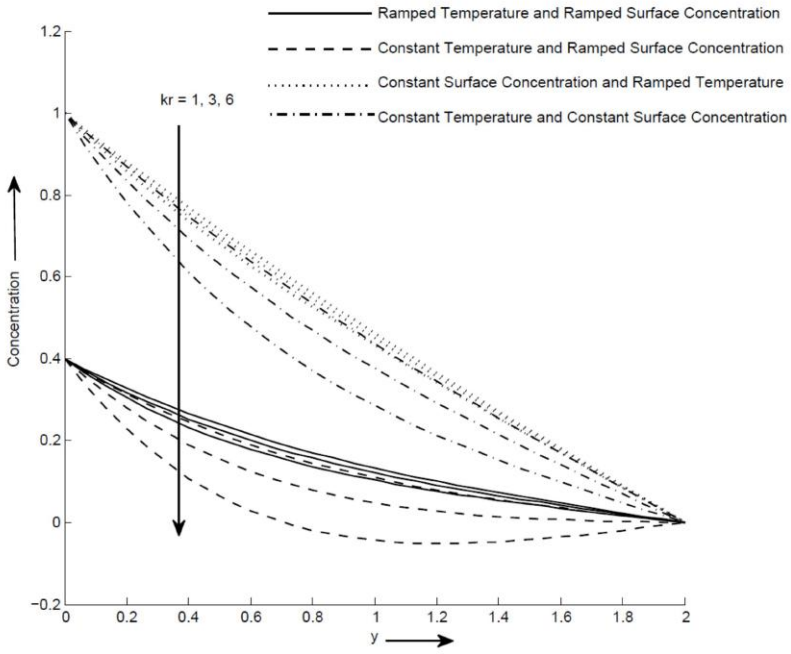

Figure 8: Concentration profile for different values of Kr and y

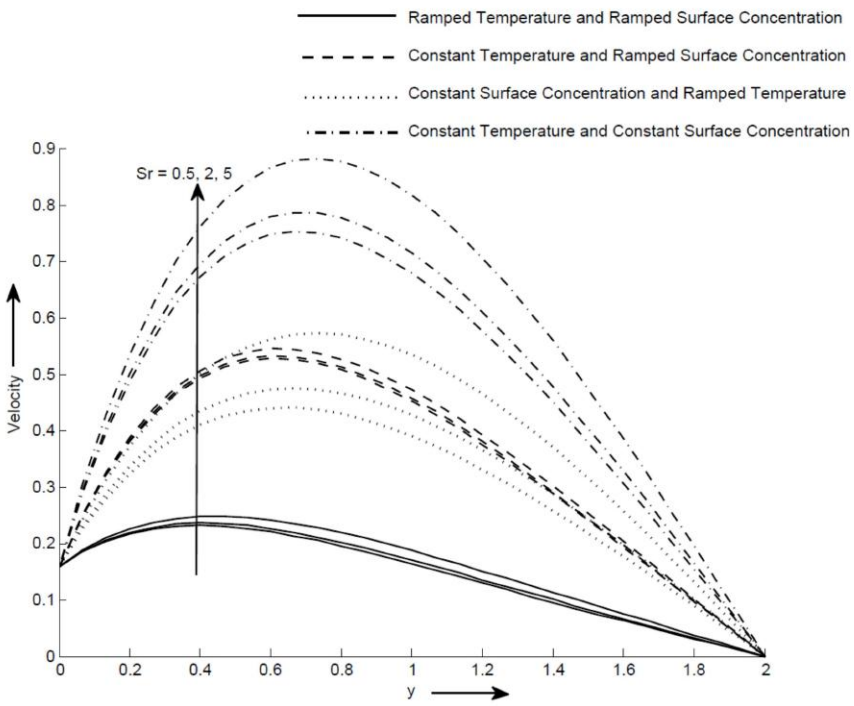

Figure 9: Velocity profile for different values of Sr and y

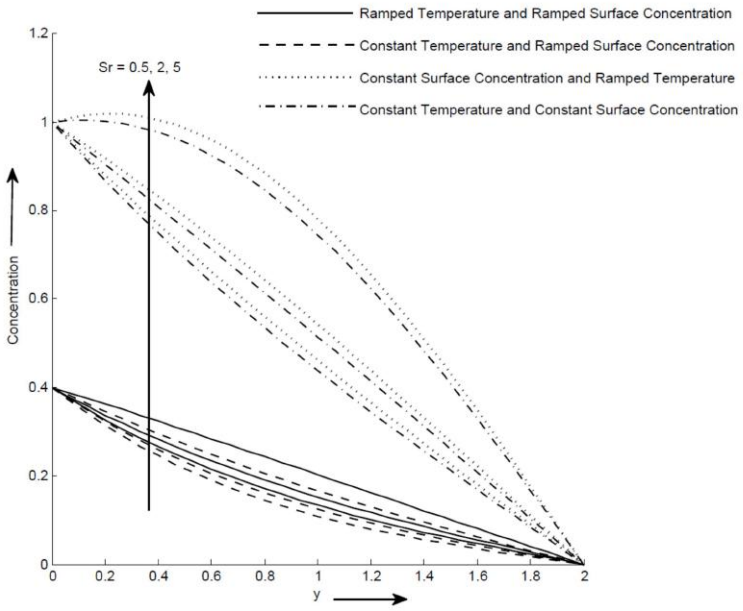

Figure 10: Concentration profile for different values of Sr and y

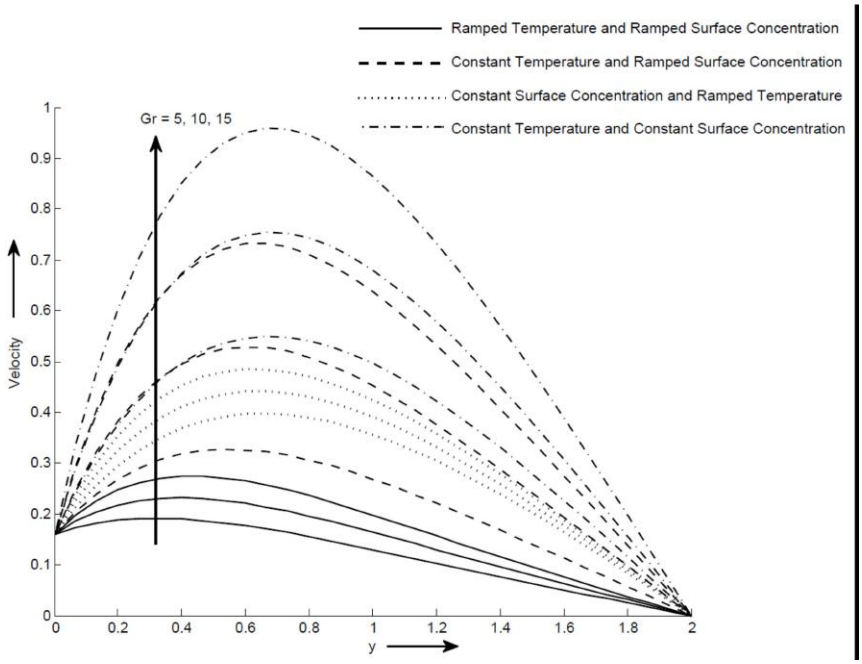

Figure 11: Velocity profile for different values of Gr and y

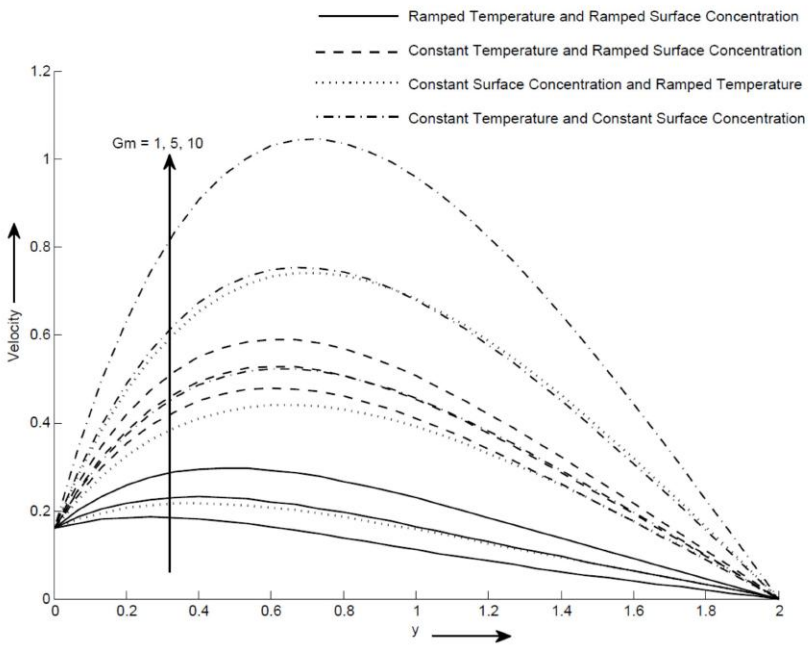

Figure 12: Velocity profile for different values of Gm and y